Renewable and Sustainable Energy Reviews 15 (2011) 1708–1721

Contents lists available at ScienceDirect

Renewable and Sustainable Energy Reviews

journal homepage: www.elsevier.com/locate/rser

The role of activated carbon fiber in adsorption cooling cycles

Dalia Attan[a], M.A. Alghoul[b,*], B.B. Saha[c], J. Assadeq[b], K. Sopian[b]

[a] UiTM Cawangan Negeri Sembilan, Kampus Kuala Pilah, 72000 Kuala Pilah, Malaysia
[b] Solar Energy Research Institute, Universiti Kebangsaan Malaysia, 43600 UKM Bangi, Selangor, Malaysia
[c] Mechanical Engineering Department, Kyushu University, 744 Motooka, Nishi-ku, Fukuoka 819-0395, Japan

ARTICLE INFO

Article history:
Received 26 May 2010
Accepted 26 October 2010
Available online 28 January 2011

Keywords:
Activated carbon fiber (ACF)
Adsorption characteristics
Adsorption cooling technology

ABSTRACT

Researches on activated carbon fiber (ACF) in adsorption cooling system are important. ACF as adsorbent offers solution to shortcomings in solar adsorption refrigeration technology. By having ACF, rapid adsorption/desorption time and higher adsorption capacity per unit mass of adsorbent can be achieved. This review paper covers and provide an up-to date research that has been devoted to advancing of various types of activated carbon fiber as adsorbent in adsorption cooling. Detailed adsorption capacity, the effect of packing density, option of adsorption cycle and various innovation of adsorbent bed employing activated carbon fiber are highlighted since these results promise heat and mass transfer improvement of the adsorbent bed. Subsequently the coefficient of performance (COP) and specific cooling effect (SCE) of adsorption cooler are improved. This particular adsorbent could help solar adsorption refrigeration technology to compete with conventional vapor compression system if its properties are further improved.

Contents

* Corresponding author.
E-mail address: dr.alghoul@gmail.com (M.A. Alghoul).

1364-0321/$ – see front matter © 2010 Elsevier Ltd. All rights reserved.
doi:10.1016/j.rser.2010.10.017

1. Introduction

Cooling is simply a process of reducing the temperature of a space or product for purposes of either comfort or preservation. It can be accomplished by various methods, using different types of energy ranging from electrical to mechanical or even purely thermal energy. Thermal energy could be fossil fuel derived, biomass derived or solar radiation [1].

The solar adsorption cooling systems are employed to meet the demands of cooling requirements such as air conditioning, ice making and medical or food preservation in remote areas. Quite, non-corrosive, environmental friendly, low cost and low maintenance of operations are the remarkable characteristics of the technology.

Adsorption capacity of working pair is an imperative indicator of adsorption cooling. High adsorption capacity results better cooling effect thus improve the performance of adsorption refrigeration. Adsorption capacity of working pair depends on the porous properties (surface area, pore size and pore volume) of the adsorbent and isothermal characteristics of the working pair.

2. Porosity standard test

Linares-Solano and Cazorla-Amoros [2] reported in their review that the evaluation of porosity of a particular adsorbent by physical adsorption of gases is the most widely used technique. Different adsorptive such as nitrogen (N_2), carbon dioxide (CO_2), Argon (Ar), helium (He), CH_4, benzene and nonane can be used for this purpose. Due to the considerable sensitivity of nitrogen adsorption isotherms to the pore structure in both microporous and mesoporous regimes and to its relative experimental simplicity of the pore structure, measurements of subcritical nitrogen adsorption at 77 K are the most used.

ACF's are highly porous materials with a fiber shape and a well-defined porous structure that can be prepared with a high adsorption capacity. The high adsorption capacity of ACF with other established adsorbent had been compared by many researchers.

Saha et al. [3,4] have compared the porous properties of silica gels, activated carbon and activated carbon fiber. Porous properties of three pitch types activated carbon fibers (ACFs), i.e. ACF (A-20), ACF (A-15) and ACF (A-10) from Unitika manufacturer company with three types of silica gels from Fuji Silysia manufacturer company (Type A^{++}, Type 3A and Type RD) are determined from the nitrogen adsorption isotherms. Standard nitrogen gas adsorption/desorption measurements of the six types of adsorbents at liquid nitrogen temperature of 77.3 K were done. ACFs have large surface areas and their adsorption/desorption rates are rapid due to the existence of numerous micropores in the vicinity of the fiber surface. Figs. 1 and 2 show the experimental nitrogen adsorption/desorption isotherm data of three types of silica gel and three types of activated carbon fibers, respectively. As the adsorption experiments are run at a temperature lower than the critical capillary condensation temperature, the adsorption theory of infinite cylinder without any external surface predicts Type IV and Type I adsorption isotherm for silica gel curves (Fig. 1) and ACF curves (Fig. 2) respectively which are characterized by solid lines for adsorption and dotted line for desorption. Characteristics features of the Type IV isotherm are its hysteresis loop, which is associated with capillary condensation, and the limiting uptake over a range of high relative pressure, P/P_s. The Type I isotherm is given by microporous solids and is concave to the P/P_s axis, and the desorption amount approaches a limiting value as P/P_s to 1. The steep region at low P/P_s is due to the filling of very narrow pores, and the limiting uptake is dependent on the accessible micropore volume rather than on the internal surface area.

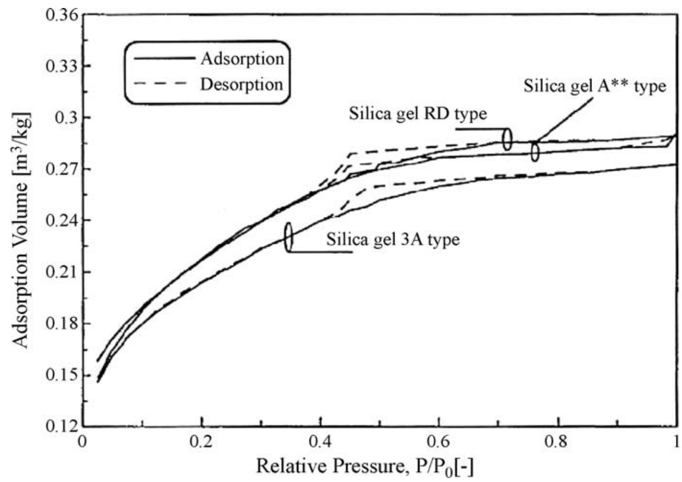


Fig. 1. The nitrogen adsorption/desorption isotherms of various silica gels. Saha et al. [3].

Fig. 1 shows that the RD type of silica gel has the highest adsorption capacity, followed by silica gel (Type A^{++}). The breakthrough curves for all three silica gels show that the adsorption and desorption branches for each gel are not superimposed on one another when the value of P/P_s is greater than 0.4, which implies the presence of adsorption/desorption hysteresis. This indicates that the silica gel isotherms are not completely reversible. However, the breakthrough curves for all three ACFs are completely reversible in the whole range of P/P_s, i.e. they do not have any hysteresis. It is also evident from Fig. 2 that the adsorption volume, which is defined as cubic meter of refrigerant per kg of adsorbent, is highest for ACF (A-20) and lowest for ACF (A-10). Comparing Figs. 1 and 2 it is evident that the adsorption capacities of all three ACFs are higher than those of silica gels. It can also be noted that the pore filling P/P_s values for all three ACFs are equal and are as low as 0.4, while for silica gel the pore filling P/P_s value lies between 0.5 and 0.7.

Measurement of the nitrogen adsorption/desorption isotherm data for activated carbon, i.e. Maxsorb III at 77.4 K is presented clearly in Fig. 3. As the adsorption experiments are run at a temperature lower than the critical capillary condensation temperature, the adsorption theory of infinite cylinder without any external surface predicts Type I adsorption isotherm for Maxsorb III, which are characterized by solid lines for adsorption and dotted lines for desorption. The type I isotherm is given by microporous solids and is

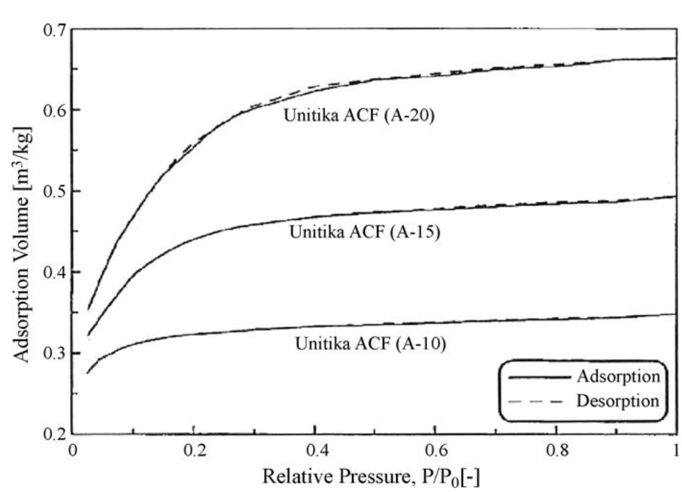


Fig. 2. The nitrogen adsorption/desorption isotherms of various carbon fibers. Saha et al. [3].

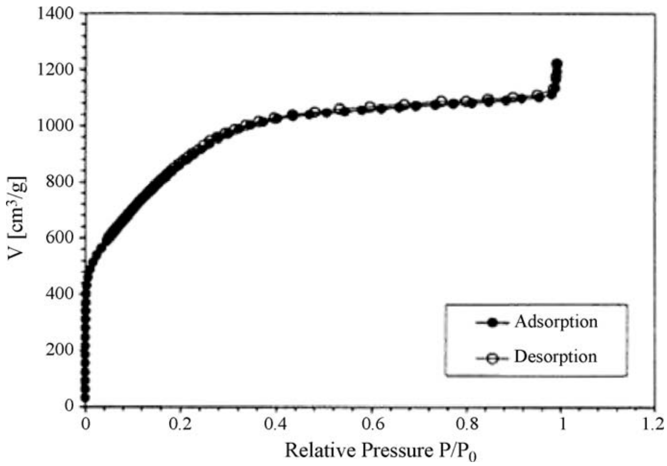


Fig. 3. The nitrogen adsorption/desorption isotherm Maxsorb III.
Saha et al. [36].

concave to the P/P_s axis and adsorption amount approaches a limiting values as P/P_s to 1. Here P_s denotes the saturated pressure of the adsorbate as shown. Saha et al. [36] reported that Ryu et al. [5] claimed that the very steep region at low P/P_s is due to the filling of very narrow pores and limiting uptake is dependent on the accessible micropore volume rather than on the internal surface area. The breakthrough curves for Maxsorb III are completely reversible in the whole range of P/P_s, i.e. they do not have any hysteresis. It is evident that the pore filling P/P_s values for Maxsorb III are equal and are as low as 0.4.

3. ACF and adsorbate

To find the best adsorbate to be worked with ACF, several refrigerants have been tested. Their suitability to be paired with ACF in adsorption process depends on the temperature lift capabilities of the working pair at adsorption–evaporation and generation and condensation temperatures [6]. This feature is important as it will determine the adsorption capacity and adsorption time of the adsorbate on the adsorbent.

3.1. ACF–ammonia

Alghoul et al. [6] reported in their review that Vasiliev et al. [7] had employed ammonia as adsorbate for ACF. Saha et al. [3] also reported that Vasiliev et al. [8] developed ACF–ammonia based solar-gas solid-sorption heat pump which managed to achieve a solar coefficient of performance of value 0.3. Vasiliev et al. [8] proposed a solar-sorption refrigerator using various types of ACFs, namely, "Busofit", which are saturated with different salts such as $CaCl_2$, $BaCl_2$ and $NiCl_2$. Ammonia was used as the refrigerant for adsorption onto Busofit.

3.2. ACF–acetone

In their review, Alghoul et al. [6] reported that Vasiliev et al. [7] implemented ACF–acetone pair for developing a refrigerator prototype.

3.3. ACF–methanol

Wang et al. [9] have presented experimental work to measure the adsorption capacity of activated carbon fibers type (ACF_0, ACF_1, ACF_2, ACF_3) and active carbon (Shanghai 18#, YK, Eshland) on methanol. The adsorbents were retreated in order to improve its adsorption capacity. The adsorption processes were executed in a vacuum condition. The data obtained show that the adsorption capacity of ACF is two or three times higher than that of normal AC tested. They found that ACF adsorbs methanol much faster than that of AC based on the isobaric measurement of adsorption capacity where AC–methanol pairs took three to four days and ACF–methanol took only 12–20 h for the adsorption process. Form the measure data, they also found that ACF needs 20 min to get 50% of the maximum capacity of adsorption, 40 min for 70%, 80 min for 90%, and 120 min for more than 95%.

Hamamoto et al. [10] have measured the equilibrium of activated carbon fiber type FX-400 and KF-1000. Both types are paired with methanol in their aim to measure the equilibrium uptake of both types with methanol. It is seen that equilibrium adsorption of both system is good at the practical operation range of relative pressure for cooling application, i.e. P/P_s values lay between 0.1 and 0.5.

3.4. ACF–water

Apart from testing ACF type KF-1000 and FX-400 with methanol, Hamamoto et al. [10] also have tested the possibility for ACF to be paired with water. From the equilibrium adsorption of ACF type KF-1000 with water, it is clarified that water is not suitable to be paired with ACF. This is because the equilibrium adsorption of this particular type at the practical operation range of relative pressure for cooling application, i.e. P/P_s values that is lay between 0.1 and 0.5 is very poor even though the latent heat of vaporization of water is higher than that of methanol.

3.5. ACF–carbon dioxide (CO_2)

Skander Jribi et al. [11] have employed carbon dioxide as refrigerant for ACF in their simulation study. An innovative CO_2 based adsorption cooling system that amalgamates the behaviors of CO_2 adsorption and desorption on activated carbon fiber type ACF (A-10) and activated carbon (Maxsorb) have been presented by them. The study is carried out to present the performances of the novel system in terms of SCE and COP for various regeneration and evaporator temperatures. The effects of regeneration temperatures on the SCE at four different evaporator temperatures namely 0, 5, 10 and 15 °C were presented for A10-CO_2 and Maxsorb-CO_2 based cooling cycles respectively. For various regeneration temperature, it is observed that higher SCE is obtained when regeneration temperatures increases. The SCE for Maxsorb is 4 times higher than A10. For the effects of regeneration temperatures on COP for Maxsorb-CO_2 and A10-CO_2 systems, they observed that the COP increases sharply at desorption temperatures below 70 °C. The COP of Maxsorb-CO_2 based adsorption cooling system is about 2 times higher than that of A10-CO_2 based system. The maximum COP of Maxsorb-CO_2 and A10-CO_2 based cooling systems are found to be 0.15 and 0.083 respectively.

3.6. ACF–gasoline vapors

Experimental investigation of adsorption equilibrium and kinetics of gasoline vapors onto activated carbon of type Maxsorb III and a felt-type activated carbon fiber (ACF-1500) have been conducted at assorted adsorbent temperatures between 20 and 60 °C. It is found that the adsorption capacity at the equilibrium condition of the Maxsorb III/gasoline pair has more than twice uptake as that of the ACF (1500)/gasoline pair. However, the experimental results show that the diffusion time constant of the ACF1500/gasoline pair is about 10 times larger than that of Maxsorb III/gasoline pair. This result implies that ACF is highly suggested for short time scale application.

3.7. ACF and ethanol

3.7.1. Adsorption capacity

From the selection of better adsorbent, Saha et al. [3] has compared the adsorption capacity of ACF (A-20), ACF (A-15) and ACF (A-10) with ethanol. The thermophysical data of these three type adsorbents were compared. Based on the comparison, the authors assumed that ACF (A-20) would have higher adsorption capacity due to its larger surface area, total pore volume and average pore diameter properties. The assumption is true based on the adsorption capacity of ACF (A-20) which shows the highest adsorption capacity compared to the other two types of ACF with the equilibrium adsorption capacity of 0.797 kg/kg.

El-Sharkawy et al. [12] compared the adsorption capacity of ACF (A-15) and ACF (A-20). The equilibrium adsorption capacity of ACF (A-20)/ethanol pair is considerably larger than that of ACF (A-15)/ethanol pair and hence it has the potential to provide higher cooling effect due to large surface area and total pore of ACF (A-20). By comparing the adsorption capacity of both adsorbent/adsorbate pairs over the pressure range of 0.2–0.5, they noticed that the adsorption capacity of ACF (A-20)/ethanol and that of ACF (A-15)/ethanol pairs are from 0.5 to 0.65 kg/kg and 0.4 to 0.45 kg/kg respectively.

3.7.2. Adsorption cooling potential of ACF

Adsorption cooling potential of ACF is determined by maximum adsorption capacity and the rate of adsorption and desorption. ACF is recommended for short adsorption–desorption cycle time. This is due to the adsorption rate of refrigerant onto ACF is mainly controlled by surface diffusion.

An experiment to measure adsorption capacity of ACF (A-20) with ethanol at assorted adsorption temperature mainly from 27 °C and 60 °C has been carried out [4,13] At adsorption temperature of 27 °C, the equilibrium uptake is achieved at 67% by mass within 47 min. At adsorption temperature of 60 °C, as expected the equilibrium ethanol uptake decreases with increasing temperatures. El-Sharkawy et al. [12] have compared the overall mass transfer coefficient with adsorption time. They deduced that the overall mass transfer coefficients increase with the increase of adsorption temperature and no significant change with adsorption time.

El-Sharkawy et al. [14] have conducted an experimental investigation on activated carbon based, i.e. Maxsorb III and activated carbon fiber with ethanol. By employing a heat source of temperature 80 °C and a coolant of temperature 30 °C, the concentration limits of ACF (A-20)/ethanol cycle are between 0.24 kg/kg and 0.58 kg/kg. It is observed that the concentration range for Maxsorb III/ethanol pairs is about 44% higher than that of the ACF (A-20)/ethanol, demonstrating the superiority of Maxsorb III/ethanol pair for cooling applications. Apart from concentration uptake, the adsorption kinetics is another essential factor that should be considered during comparison between two different adsorbent–adsorbate pairs. From the change of fractional uptake versus time graph of the Maxsorb III–ethanol and that of ACF (A-20)–ethanol pair at a constant adsorption temperature of 30 °C, it is seen that the adsorption rate of ACF (A-20)–ethanol pair is much faster than Maxsorb III–ethanol pair at adsorption temperature 30 °C. This is due to the short diffusion path of ACF particles compared to that of granular shapes adsorbents thus give an implication that ACF might be suitable for waste heat powered adsorption cooling application where short adsorption–desorption cycle time of around 5–10 min is anticipated.

3.7.3. Bed apparent density

As adsorption chiller need to be in a compact size, reduction of size each of component is important. Adsorbent material that can be compressed without reduction in performance is what researches looking forward.

Adsorbent bed that can be compressed offer a reduction size of adsorption chiller. In doing so, that particular adsorbent material should have higher packing density for refrigerant storage. ACF which has fiber shape with small diameter offer this property. As the ACF bed is compressible, mass of adsorbent per cubic meter depends on the degree of packing. Bed apparent density of ACF is defined as the mass of ACF that can be packed in a unit volume (cubic meter).

Another remarkable option that ACF can be packed is as this is not only offer size reduction but also the adsorbent bed manage to have a higher regeneration temperature as the packing density is increasing. It also found that, higher packing density increases the specific cooling effect of adsorption chiller.

El-Sharkawy and coworkers [15] has studied the effect of regeneration and evaporator temperatures on cooling effect per unit volume at various bed apparent density. They also analyzed the relationship between the cooling effect, COP and adsorbent bed apparent density. They found that specific cooling effect increase linearly by the increase of regeneration temperature. Cooling capacity per unit volume also increases with the increase of evaporator and regeneration temperature. Cooling capacity per unit volume increases with the increase of adsorbent bed apparent density, which may lead to design a compact adsorption unit.

Koyama Shigeru et al. [16] made a study deals with ACF/ethanol adsorption equilibrium examination and one-dimensional transient numerical simulation. This study considered the relationship between cooling capacity and system conditions such as system temperature and apparent density and suggests optimizing method for performance improvement.

El-Sharkawy et al. [12] found that by comparing the adsorption capacity of both ACF (A-15)/ethanol and ACF (A-20)/ethanol pairs over the pressure range of 0.2–0.5, apart from larger adsorption capacity of ACF (A-20), they noticed that for the same apparent density of the adsorbent bed, ACF (A-20) can provide higher cooling effects. The authors also summarized that adsorption rate per cubic meter of adsorber increases with increasing bed apparent density. The experimental data show that at apparent density of 50 kg/m^3, ACF (A-20) can be saturated by ethanol in only 40 min. However, the required time to reach equilibrium is about 60 and 100 min for apparent densities of 100 and 150 kg/m^3 respectively. On the other hand, the mass of ethanol adsorbed per unit volume of the adsorber increases with increasing bed apparent density at the beginning of adsorption process to reach its maximum value at apparent density of 100 kg/m^3. Therefore, by increasing the bed apparent density, mass of refrigerant adsorbed per unit volume increases, which may lead to the design of compact adsorption unit.

Saha et al. (2006)[17] have presented a numerical investigation on the performance of a thermally driven two-stage adsorption chiller where low grade waste heat sources between 50 °C and 70 °C are employed in combination with a heat sink (cooling water) of 30 °C. Activated carbon fiber (A-20)/ethanol pair has been examined as working pair. A cycle simulation program is developed to analyze the influence of operating conditions (hot and cooling water temperatures and adsorption/desorption cycle times) on the cycle performance in terms of cooling capacity and COP. The main advantage of this two-stage chiller is that it can be operational with smaller regenerating temperatures lifts ($T_{\text{regeneration}} \geq$ heat source – heat sink inlet temperatures) than other heat-driven single-stage chillers. Being a compressible material, the effect of packing density of ACF in the adsorbent beds is also considered in the present model. Simulation results shows that the two-stage chiller can be operated effectively with heat sources of 50 °C and 70 °C in combination with a coolant at 30 °C.

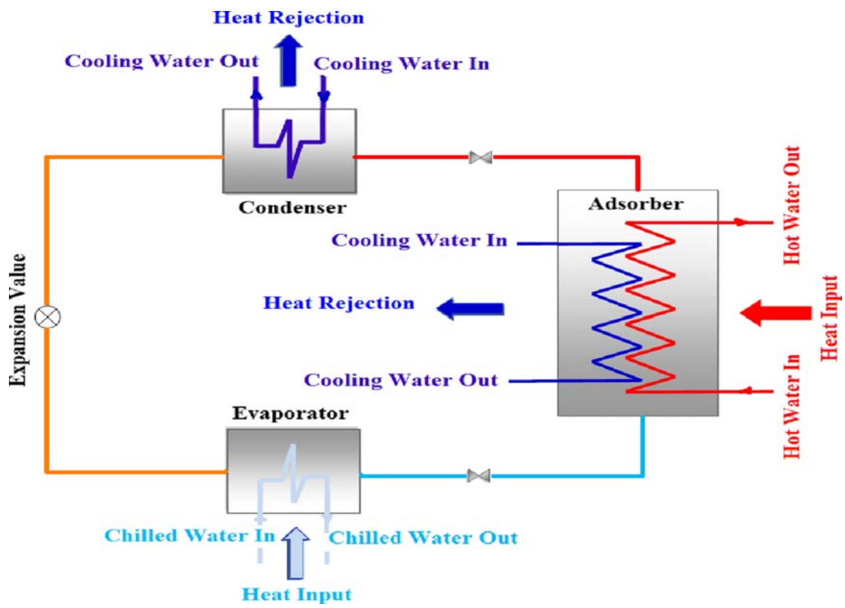


Fig. 4. The schematic diagram of system.

Skander Jribi et al. [11].

Kariya Keishi et al. [18] made a study deals with the experimental investigation of ethanol vapor adsorption on activated carbon fiber (ACF) under equilibrium condition along with one-dimensional transient numerical simulation of heat and mass transfer in the adsorbent bed is also performed. In order to suggest optimizing method for performance improvement, the present study considered the relationship between cooling capacity and system performance including parameters, such as cooling water temperature, ACF height and apparent density in the simulation model. Simulation results agreed well with the experimental data and it is found that the cooling capacity can be enhanced by optimizing ACF bed thickness. Simulation results also show that the temperatures of adsorber and evaporator do not have significant effects on the optimum adsorption cycle time.

Loh et al. [19] found that, although the silica gel/water pair is found to be the most feasible adsorbent/adsorbate pair among the six assorted adsorbent/adsorbate pairs, increasing the packing density of ACF (A-20) in the reactor beds may lead the ACF (A-20)/ethanol based adsorption cooling systems promising for cooling application.

4. ACF in adsorption cooling cycle

4.1. Types of cycle

Works employing activated carbon fiber as adsorbent in adsorption cycle has been reported. Up to now, more research is focused on the single purpose adsorption compared to dual purpose adsorption. Simulation and experimental studies has been carried out to analyze the performance developed.

An innovative CO_2 based adsorption cooling system that amalgamates the behaviors of CO_2 adsorption and desorption on activated carbon fiber type ACF (A-20) and activated carbon (Maxsorb) have been presented [11]. This study is carried out to present the performances of this novel system in terms of SCE and COP for various regeneration and evaporator temperatures as shown in Fig. 4. These two cooling systems were simulated for the driving heat source temperatures ranging from 30 °C to 90 °C in terms of different cooling load temperatures with a cooling source temperature of 25 °C. The effects of regeneration temperatures on the SCE at four different evaporator temperatures namely 0,5,10 and 15 °C were presented for A10-CO_2 and Maxsorb-CO_2 based cooling cycles respectively. For various regeneration temperature, it is observed that higher SCE is obtained when regeneration temperatures increases. The SCE for Maxsorb is 4 times higher than A10. For the effects of regeneration temperatures on COP for Maxsorb-CO_2 and A10-CO_2 systems, they observed that the COP increases sharply at desorption temperatures below 70 °C. At desorption temperature above 70 °C, the increase in COP is marginal even though the SCE increase. The COP of Maxsorb-CO_2 based adsorption cooling system is about 2 times higher than that of A10-CO_2 based system. The maximum COP of Maxsorb-CO_2 and A10-CO_2 based cooling systems are found to be 0.015 and 0.083 respectively. For this particular system, the continuous cooling operation, a low pressure CO_2 is evaporated at the evaporator due to the external cooling load and is adsorbed into the solid adsorbent located in the adsorber at evaporator pressure (P_e). The process of adsorption results in the liberation of heat of adsorption at the adsorber providing a useful heat energy output and a cooling effect in the condenser/evaporator heat exchanger. Secondly, the adsorbed bed is heated by the external heat source and the refrigerant is desorbed from the adsorbent and goes to the condenser at condenser pressure (P_c) for condensation by pumping heat through the environment. The refrigerant is refluxed back to the evaporator via a pressure reducing valve for maintaining the pressure difference between the condenser and the evaporator. Pool boiling is affected in the evaporator by the vapor uptake at the adsorber thus completing the refrigeration cycle.

Loh et al. [19] had simulated performances for six working pairs, i.e. ACF (A-15)/ethanol, ACF (A-20)/ethanol, silica gel/water, Chemviron/R134a, Fluka/R134a and Maxsorb II/R134a. Performance of each working pairs in terms of COP and SCE in single effect double lift and single stage cycle at partial vacuum and pressurized conditions have been compared. A pair of adsorber bed were employed in single stage cycle and 2 pairs of adsorbent bed were employed in single effect double lift cycle where each bed in single effect double lift cycle carry only half the amount of adsorbent of the adsorbent bed in single stage adsorption cycle. ACF (A-20)/ethanol pair can achieve a specific cooling effect of 344 kJ/kg and COP of 0.68 at a regeneration temperature of 85 °C in single stage mode and SCE of 228.2 kJ/kg and COP of 0.38 in single effect lift mode. For

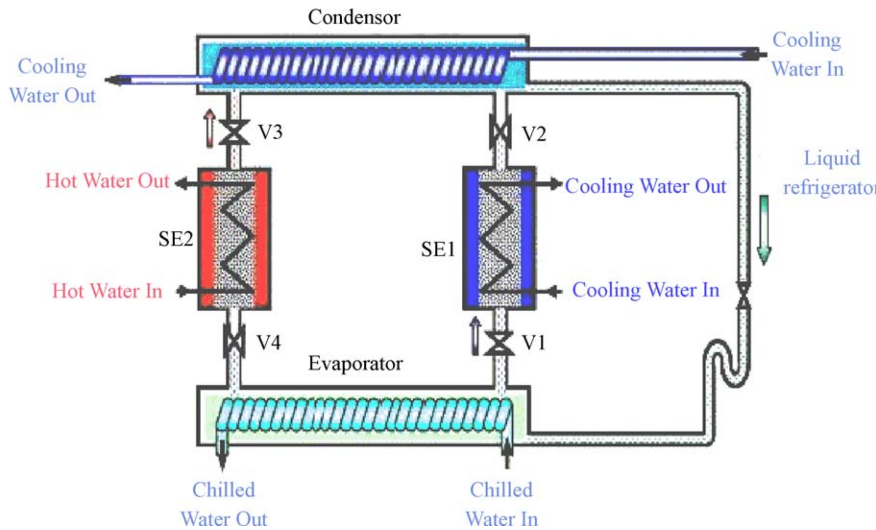


Fig. 5. The schematic diagram of the two-bed AC–ethanol adsorption cycle (Mode A).

Saha et al. [20].

single stage and single effect double lift cycles, ACF (A-20)/ethanol provides the highest value for SCE.

Saha et al. [20] presented a simulation modeling for a two bed, ACF ethanol adsorption chiller. The aim of the simulation was to investigate the performance of a two-bed, non-regenerative of the working pair. A cycle simulation computer program of the innovative system was meant to analyze the cooling capacity and COP variations by varying the heat transfer fluid (hot, cooling and chilled water) inlet temperatures, the heat transfer fluid flow rates, the cycle time and the switching time.

The schematic of the two-bed ACF–ethanol cycle is shown in Figs. 5 and 6. The cycle consists of four heat exchangers, evaporator—sorption element 1 (SE 1) and condenser—sorption element 2 (SE 2). The operation cycle has four modes, Mode A, B, C, and D. In Mode A as shown in Fig. 5, valves V1 and V3 are opened, while valves V2 and V4 are closed. In this mode, evaporator and SE 1 is in adsorption process and condenser and SE 2 is in desorption process. In the adsorption–evaporation process which takes place at pressure, P_{evap}, ethanol in evaporator is evaporated at evaporation temperature, T_{evap} and seized heat, Q_{evap} from the chilled water. The evaporated vapor is adsorbed by activated carbon fiber, at which cooling water removes the adsorption heat, Q_{ads}. The desorption–condensation process takes place at pressure P_{cond}. Then, the desorber (SE 2) is heated up to the desorber temperature T_{des} which is provided by the driving heat source Q_{des}. The resulting ethanol vapor is cooled down to temperature T_{cond} in the condenser by the cooling water, which removes condensation heat, Q_{cond}. When the refrigerant concentrations in the adsorber and the desorber are at or near their equilibrium levels, the cycle is continued by changing into a short duration (30 sec) named pre-heating or pre-cooling mode (Mode B), where all refrigerant valves remain closed. In Mode B, heat transfer fluids (hot and cooling water) flows are redirected to ensure pre-heating and pre-cooling process of SE 1 and SE 2, respectively. When the pressures of desorber and adsorber are nearly equal to the pressures of condenser and evaporator, respectively, then valve between SE 2 and evaporator, as well as the valve between SE 1 and condenser are opened to flow the refrigerant. This mode is denoted as Mode C. In Mode C, valves V2 and V4 are opened, while valves V1 and V3 are closed. In this mode, the condenser and the SE 1 is in desorption process and the evaporator and the SE 2 is in adsorption process. As can be noticed from Fig. 6 and Table 1, in Mode C, all four refrigerant valve's operations and the processes of SE 1 and SE 2 are exactly opposite to those of Mode A. After the completion of Mode C, pre-heating of SE 2 or

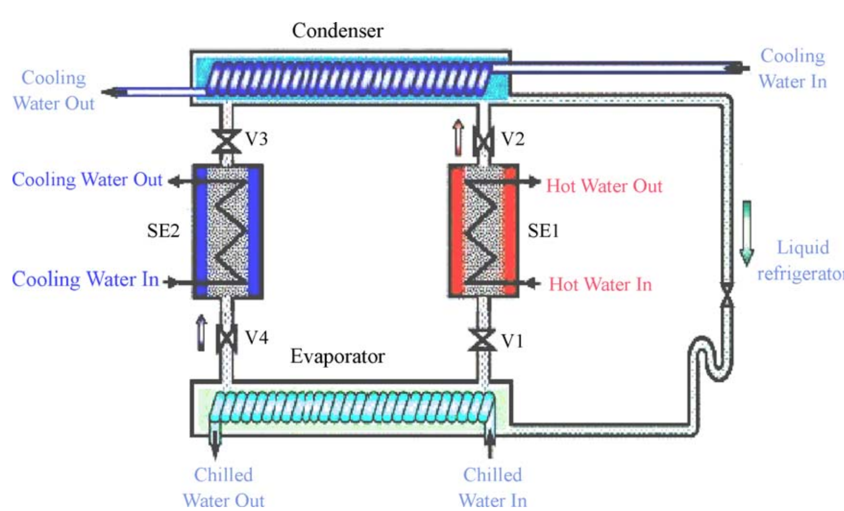


Fig. 6. The schematic diagram of the two-bed AC–ethanol adsorption cycle (Mode C).

Saha et al. [21].

Table 1
Operation mode of refrigerant valves and sorption elements.

Cycle (duration)	Mode A (600 s)	Mode B (30 s)	Mode C (600 s)	Mode D (30 s)
Valve 1	Open	Closed	Closed	Closed
Valve 2	Closed	Closed	Open	Closed
Valve 3	Open	Closed	Closed	Closed
Valve 4	Closed	Closed	Open	Closed
SE 1	Cooling water	Hot water	Hot water	Cooling water
SE 2	Hot water	Cooling water	Cooling water	Hot water

pre-cooling of SE 1 starts, which is opposite of Mode B and known as Mode D. After Mode D, the adsorption cooling system returns to Mode A. Table 1 shows the state of the refrigerant valves and the choice of hot or cooling water application.

The main advantage in the ACF–ethanol adsorption cycle is its ability to utilize effectively low-temperature waste heat between 60 and 95 °C as the driving heat source and heat sink temperature difference as small as 30 °C. Cooling capacity increases with higher driving sources temperature along with a fixed coolant temperature. With cooling water temperature at 30 °C an optimum COP values are obtained with driving source temperatures between 85 and 95 °C. The performance of the chiller increases with the increase of hot, cooling and chilled water flow rates. However, flow rates of hot or cooling water above 1.5 kg/s and the chilled water flow rate above 0.7 kg/s results a marginal improvement. The optimum cooling capacity were recorded for cycle time at 600 s with a preheating or precooling cycle time and switching time between 30 and 50 s.

Hamamoto et al. [22] investigate the system performance of an adsorption cycle by having adopted ACF (FX-400)/methanol as working pair in their simulation study. The schematic of ACF based single stage adsorption cycle is shown in Fig. 7. It consists of four heat exchangers, namely an evaporator, an adsorber, a condenser and a desorber. ACF is packed into the two adsorber/desorber heat exchangers. The SCE and COP of the system are evaluated from the adsorption equilibrium theory with different hot, cooling and chilled fluid inlet temperatures. There is an optimum condition for COP to reach at maximum for this particular working pair. Particularly, the working pair system shows better performance with lower chilled fluid inlet temperature between −20 and 20 °C at the same inlet temperature difference between cooling and chilled fluids.

The authors then proposed an advanced cascaded cycle as shown in Fig. 8. The advanced cascaded cycle is composed of two different adsorbents, i.e. silica gel and ACF to achieve higher COP with hot fluid inlet temperature at 80 °C, cooling fluid at 30 °C and chilled fluid at −20 °C. This advanced cascaded system is composed of the silica gel system as the first stage cycle, and ACF as the second stage cycle. Chilled fluid from silica gel system is used as cooling fluid for ACF system. For instance, in first stage, silica gel system is operated with hot fluid of 80 °C, cooling fluid of 30 °C and delivered chilled fluid of 10 °C. The obtained chilled fluid of 10 °C is supplied to ACF system as the cooling fluid. In the second stage, ACF system is operated with hot fluid of 80 °C, cooling fluid of 10 °C and chilled fluid of −20 °C. From the data, the recorded COP of silica gel system was 0.38 and COP of the COP of ACF was 0.27 and the total COP was 0.062. If only silica gel were employed in both stages, COP recorded was 0.044, indicating that total COP of the advanced cycle is 40% higher than that of silica-gel based cascade cycles. If both stages are operated with ACF as adsorbent, the COP becomes 0.047, which is 30% lower than that of advanced cycle. Up to now, only one experiment employing ACF in dual purpose adsorption system [23].

A solar powered hybrid adsorption ice maker with ACF–methanol as the working pair had developed and shown in Fig. 9 [23]. The schematic in Fig. 9 is for a dual purpose solar water heater and ice-maker. The system consists of double glazed evacuated vacuum tube type collector, water tank, 10 stainless steel tube adsorber, water storage tank, fin type condenser, evaporator and valves. Their analysis indicated that for a given amount of adsorbent/adsorbate, by adapting more adsorbers instead of conventionally used single adsorber bed as shown in Fig. 10 [23], the performance of the system can be enhanced. Apart from the number of adsorber module, condensing, evaporating and adsorption temperatures, collector area and mass of water influence their system performance.

The optimization was achieved by having evacuated vacuum tube type collector, with an exposed area of 2.0 m^2 at adsorption

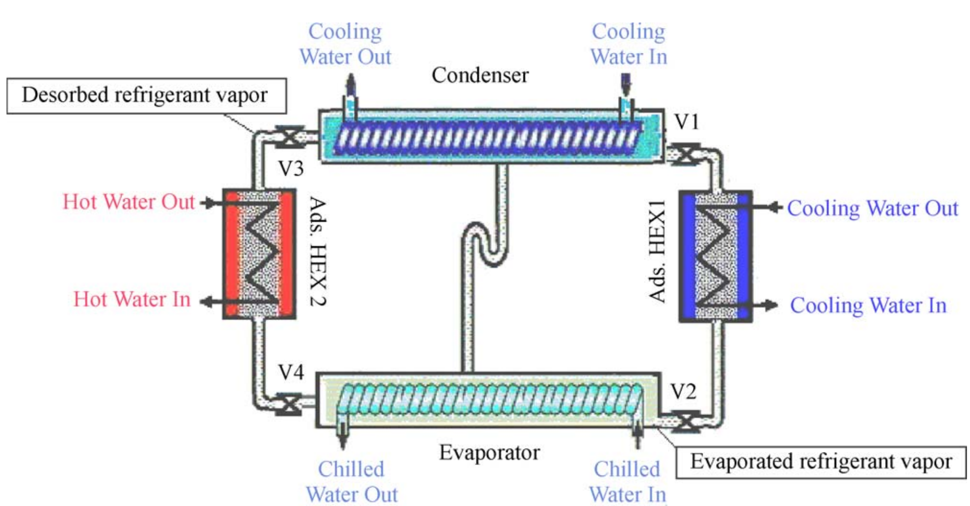


Fig. 7. The schematic diagram of the single-stage adsoption chiller.

Hamamoto et al. [22].

temperature 35 °C, desorption temperature 90 °C, evaporation temperature −5 °C and condensation temperature 30 °C. This system manages to have a COP of about 0.56 and capable to produce 6.2 kg of ice a day.

During the day, the solar energy in the collector is accumulated in the water tank and the hot water in the tank raises the temperature in the adsorbent bed. As the temperature bed increases, desorption and evaporation of the refrigerant are started. With the progressive heating of the adsorbent, the refrigerant continues to desorb until the adsorbent reaches its maximum temperature. At this temperature, desorption ceases and the evaporated adsorbate is then cooled by the condenser and the liquid adsorbate finally is transferred and stored in the evaporator to complete the regeneration of the ACF.

During the night, the hot water is drained and stored in the water storage tank temporarily or used directly for domestic purposes and the cold water is filled in the water tank. The cold water cools down the adsorber quickly, and the cooling–adsorption–evaporation process can thereby be initialized so that the sensible heat of the adsorber and heat of adsorption will preheat the cold water in the tank. This heat recovery process is important since the solar energy gained from the collector can be effectively utilized. When the adsorber temperature decreases, the system pressure decreases to the evaporation pressure, P_E. During this period, the liquid adsorbate in the vaporator begins to evaporate by adsorbing heat energy from water stored in the evaporator and gets adsorbed by the adsorbent in adsorber. During this process, the water in the evaporator cools and ice is produced.

4.2. Adsorber bed design

Aiping Zheng and Juan Gu [25] had innovated a novel design of adsorber bed. Instead of using two or more adsorbers to improve heat and mass transfer performance of refrigerant, they had adopted rotary ACF adsorbing bed which utilizes ethanol as the adsorbate. The rotary heat pump machine consist mainly of adsorbent bed, a condenser, an evaporator, a throttling valve, and a solar energy heater which composed of vacuum pipe heat collector and auxiliary heating devices, etc. The operation principle of the systems is shown in Fig. 11.

In this particular system, the low pressure of refrigerant vapor with low temperature from evaporator is introduced to the 3/5 area of the bottom part of the rotary adsorbent bed by the gas circulation pump. This will make the adsorbent bed temperature drop first and refrigerant vapor will be adsorbed by the ACF. During this process, heat released from the adsorption process will be taken away by refrigerant vapor that is not adsorbed by ACF and will be flow to solar energy heater orderly. The refrigerant vapor not adsorbed by the adsorbent bed will be heated by the solar energy heater and then it will adsorb heat and increase the temperature slightly. The heated refrigerant will then enter the 2/5 area of the upper part of the rotary adsorbent bed after its pressure rising enough, then it

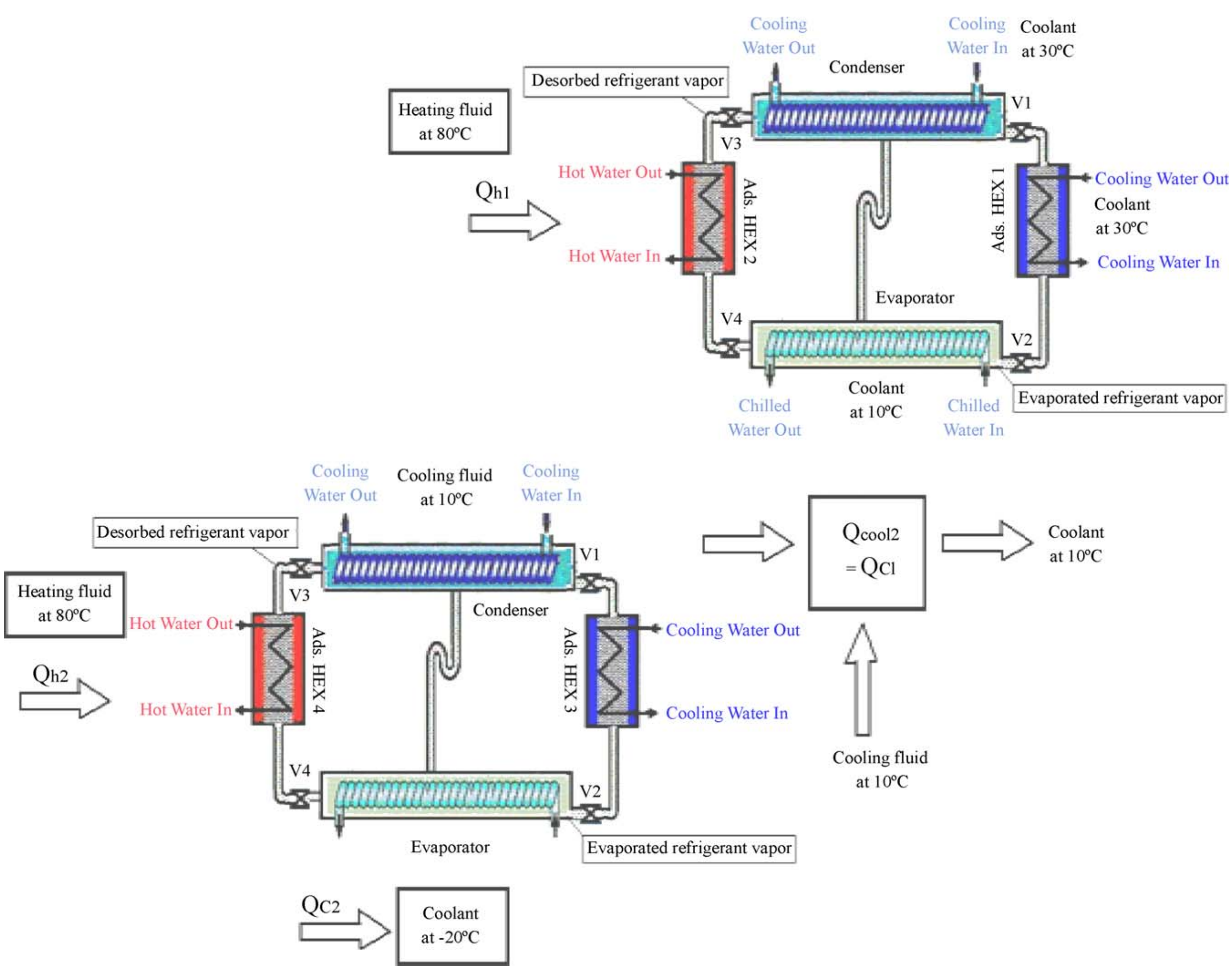


Fig. 8. The schematic diagram of advanced cascaded adsorption cycle.

Hamamoto et al. [22].

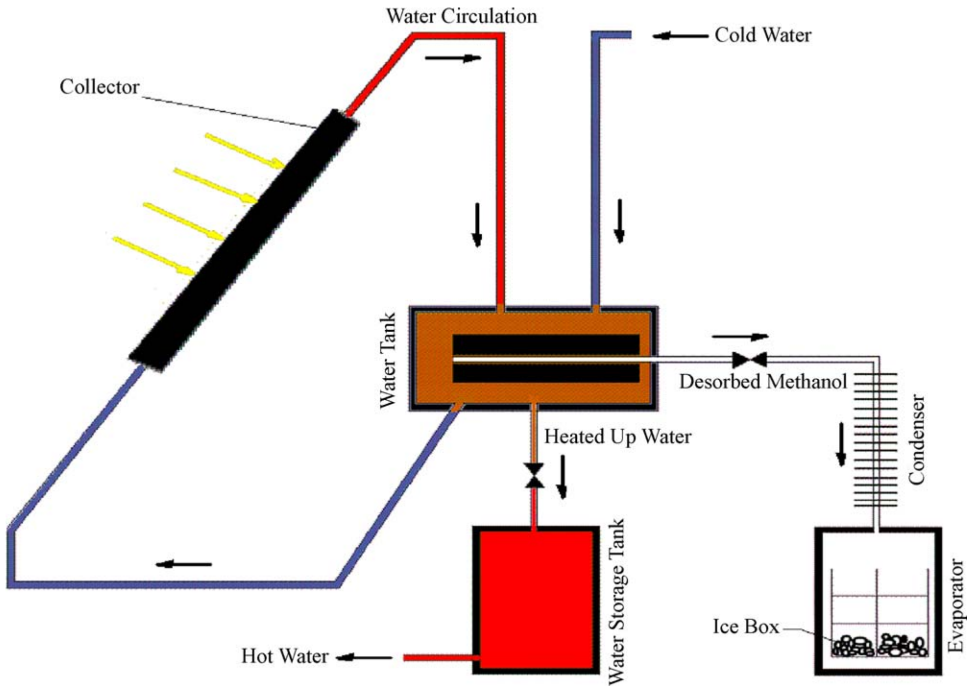


Fig. 9. Schematic of the dual purpose adsorption system.
Yeung and Sumathy [23].

will meet the adsorbent bed layer rotating up which had adsorbed refrigerant. Because the refrigerant adsorbed by the adsorbent bed will be heated by the high temperature refrigerant vapor, then it will be desorbed from the ACF, afterwards, it enters the condenser and will be cooled by the cooled water and condensate into liquid refrigerant. After being throttled and the pressure reduced, the liquid adsorbate will enter the evaporator. In the evaporator, the low pressure adsorbate liquid will adsorb the heat from the cooled medium, and then it will be gasified into refrigerant vapor. Because the cooled medium has lost heat, it will generate the cooling effect after its temperature decreasing. Then the low pressure refrigerant vapor of low temperature will be channeled into the 3/5 area of the bottom part of the rotary adsorbing bed by the gas pump again and repeat the cycle.

The rotary adsorbing is the key device of the components of the system developed. It consists of rotary ACF, outer cover, transmission device, etc., as shown in Fig. 12. The ACF wheel is made by the metal net boards knotted by the ACF felt, 4 mm thickness and arranged in the center of the wheel with radiation form. The wheel is rotated at a slow speed, the low pressure refrigerant vapor with low temperature coming from evaporator enters each channel of the bottom 3/5 area part of the wheel through the right end of the gas pump.

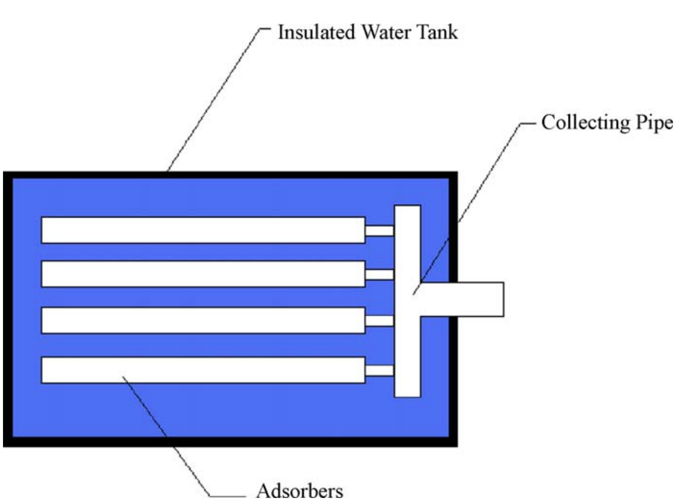


Fig. 10. Section of the adsorbent bed.
Yeung and Sumathy [23].

In their aim to find the best working pair to be operated in the system, ACF–ethanol appeared as the best working pair compared to the other 3 working pairs, i.e. silica gel/water, activated carbon/ammonia, activated carbon/methanol. For ACF–ethanol pair, the condenser temperature of 303 K, evaporator temperature 268 K and adsorption temperature 303 K and desorption temperature 373 K gives uptake capacity of 0.145 and COP of 0.85.

Saha et al. [3] have measured the adsorption characteristics of ACF/ethanol pair using a plate-fin heat exchanger. They developed an intermittent adsorption refrigeration system using an ACF (A-20)/ethanol pair. Experiments are performed to determine the temperature and pressure profiles, along with the various heat transfer rates and overall heat transfer coefficient during preheating and desorption process of the reactor bed, which play an important roles in cooling system performance. A photograph and specification of the adsorber/desorber heat exchanger is shown in Fig. 13.

The adsorber/desorber heat exchanger is a plate-fin heat exchanger which is made of oxygen-free copper material. The heat exchanger is 402 mm in length, 200 mm in width, and 38.6 mm in height. Fin height, fin pitch and fin thickness are 15 mm, 6 mm and 2 mm respectively. ACF (A-20) fibers are packed tightly inside the fins and are covered by carbon fiber based fine mesh net.

The diagram of the experimental apparatus is shown in Fig. 14. The test rig consists of a sorption element (adsorber/desorber heat exchanger), a condenser, an evaporator, one refrigerant tank, and four mixing chambers along with six manually operated valves.

As adsorption/desorption occurs at sub atmospheric pressure for an ACF/ethanol system, the test section is connected to a vacuum pump. In order to attain near zero pressure in the sorption

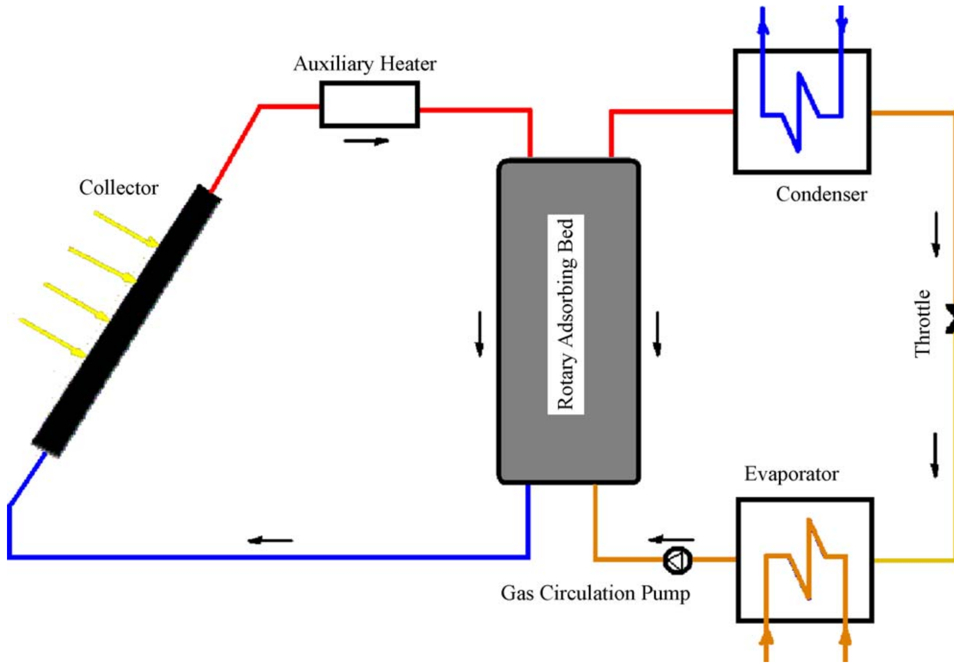


Fig. 11. The operation principle of rotary solid adsorption refrigerator.
Aiping Zheng and Juan Gu [25].

element (SE), depressurization for an hour in the adsorber/desorber heat exchanger is done by the vacuum pump. Two water circulators are connected with the sorption element to provide either cooling water or hot water inside the heat transfer tube of the sorption element according to its operation modes (cooling water during adsorption and precooling modes or hot water during desorption and preheating operations). The evaporator, the condenser and the test section are thermally insulated perfectly to avoid external heat losses. Ambient temperature is kept at the temperature level of the cooling water. During adsorption, the valve between the sorption element and the condenser is kept closed manually while the valve between the evaporator and sorption element is kept open. Ethanol vapor from the evaporator goes to the sorption element. Temperature and pressure profiles of the sorption element along with various heat transfer rates are measured experimentally. During desorption, the valve between the SE and condenser is kept open while the valve between the evaporator and sorption element is kept closed. Desorbed vapor goes to the condenser, and the condensation heat is removed by the coolant. Liquefied refrigerant returns back to the evaporator via the capillary tube connecting between the condenser and evaporator. It is observed that, adsorption occurs rapidly during the first 500 s of the adsorption cycle. As a result, temperature rises sharply in that particular period due to the release of adsorption heat. After that, adsorption occurs slowly as it reaches near the equilibrium level. Adsorption heat is removed by the cooling water.

The overall desorption heat transfer coefficient increases abruptly in the initial 50 s, reaches a maximum value of 1780 (W/m^2 K) and after that starts to decrease. The sorption element average overall desorption heat transfer coefficient values are 500 W/m^2 K and 112 W/m^2 K for desorption cycle times of 100 s and 1000 s, respectively. Based on this result, the authors proposed short adsorption/desorption cycle in order to attain high performance.

Similar type of heat exchanger also had been developed by Takao Kashiwagi et al. [26]. The authors carried out an experimental investigation of a plate-fin heat exchanger using ACF/ethanol as working pair. The fin pitch, fin thickness and fin height are taken as 8 mm, 2 mm, and 15 mm, respectively. In the design, the total length of the heat transfer fluid (HTF) is taken as 5 m in order to obtain high temperature difference between HTF inlet and outlet.

The overall heat transfer coefficient of this particular experiment also exhibit the same character like the one designed by

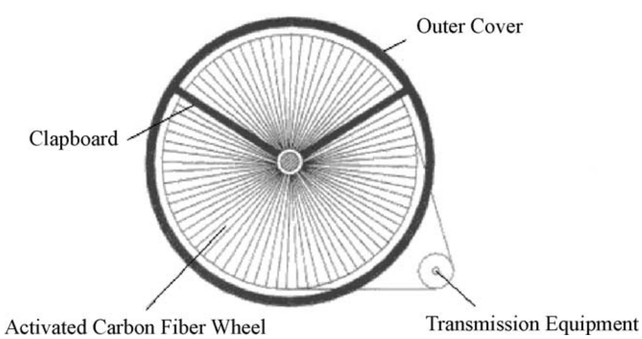


Fig. 12. Rotary activated carbon fiber adsorbing bed.
Aiping Zheng and Juan Gu [25].

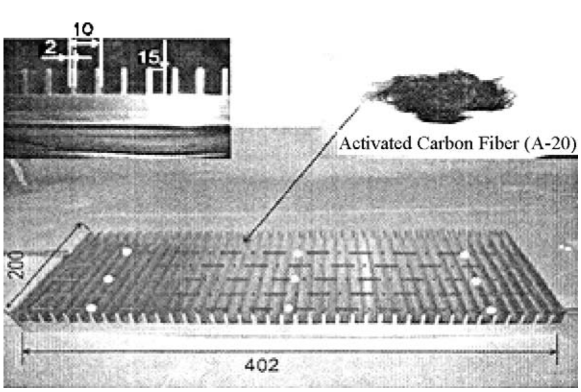


Fig. 13. Photograph and specification of the plate-fin heat exchanger.
Saha et al. [3].

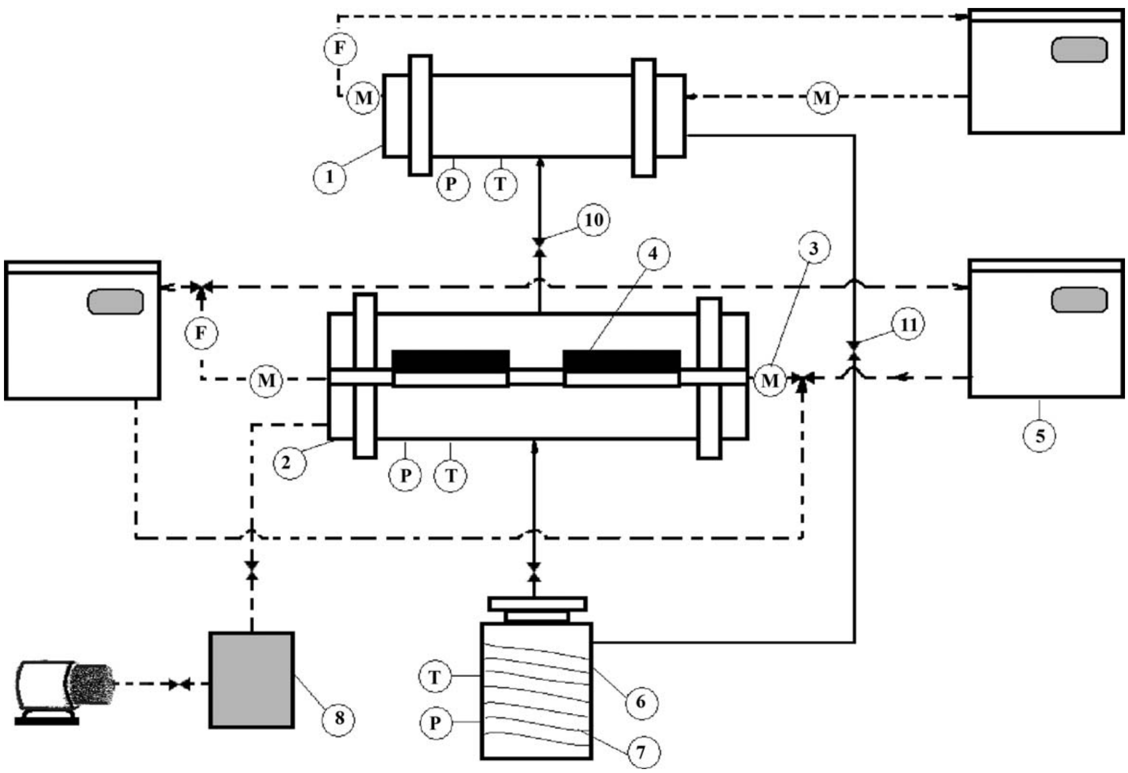


Fig. 14. The schematic diagram of the intermittent ACF/ethanol adsorption refrigeration system Saha et al. [3].

Saha et al. [3]. The heat transfer coefficient is maximum at 50 s after the starting of the desorption mode. The average net adsorption heat transfer coefficient during the first 80 s is around 1000 W/m^2 K. However, the average net desorption heat transfer coefficient is as low as 5 W/m^2 K during 500 to 2000 s which means short cycle is important to have high performance.

Koyama Shigeru et al. [27] made a study deals with two dimensional numerical simulations to clarify adsorption characteristics in the plate-fin and tube type adsorber heat exchanger during adsorption process using activated carbon fiber (ACF) of type (A-20) and ethanol pair. They found that the cooling capacity can be enhanced by optimizing fin pitch. Simulation results also show that cooling capacity increase with the increase of fin (ACF) height and the decreasing of fin thickness.

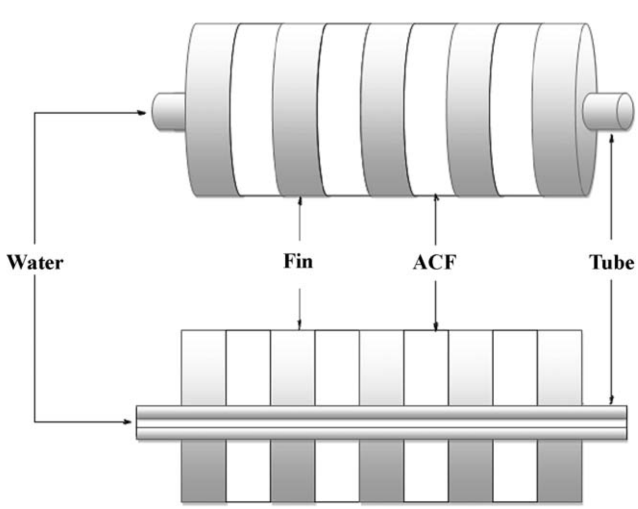


Fig. 15. The round fin and tube type adsorber. Keishi Kariya et al. [28].

For round fin and tube type adsorber (as shown in Fig. 15), Keishi Kariya et al. [28] have analyzed the cooling capacity and optimum adsorption cycle time of an adsorber employing ACF/ethanol as working pair. The simulation study covers the effects of the local heat and mass transfer as well as the fin geometry of the heat exchanger. The adsorption performance of this particular adsorber type have been determined by varying parameters, i.e. ACF bed apparent density, fin thickness, fin pitch, fin height and tube diameter along with evaporator and cooling water inlet temperatures. There is an optimum condition for COP to reach at maximum. The results show that the adsorption performances increase by optimizing the tube diameter, fin height and fin pitch. Maximum cooling capacity was achieved when fin height is 15 mm and fin pitch is 5 mm when other parameters are kept fixed. It is observed that, the cooling capacity decreases with the increase of adsorber tube diameter and the tube diameter give marginal influence on the optimum cycle time. The optimum cycle time increase with the increase of fin height and decrease of fin pitch [28].

5. ACF composite

5.1. ACF composite adsorbent

Chemical adsorbents are another type of adsorbent employed in solar adsorption refrigeration. However, the swelling and agglomeration occurrence in the adsorption process hurdles the practicality to utilize this particular adsorbent type. Therefore, composite adsorbents are introduced to handle these two shortcomings.

According to Wang et al. [29] and Han and Lee [30] found that composite adsorbents are utilized specifically to improve heat and mass transfer performance of chemical adsorbents due to swelling

and agglomeration phenomena. Salt swelling reduces the heat transfer and salt agglomeration reduces the mass transfer. Thus, the additive (physical adsorbent) for chemical adsorbents should have a high porous structure and high thermal conductivity. In addition, the adsorption quantity of physical adsorbents can be increased if the adsorbents were employed.

Employment of ACF as additive in composite adsorbents promises a bright future. The adsorbent has highly porous structure and better thermal conductivity which lead to solution for swelling and agglomeration phenomena.

Dellero et al. [31] had utilized ACF to enhance their chemical heat pump performance. In doing so, they proposed three ways to stick the carbon fibers to the reagent compounds, i.e. simple mixture, impregnated carbon fibers and intercalation graphite fiber compounds and compared 6 compounds in their aim to find the best composite which can enhance the system performance.

The compounds tested were pure $MnCl_2$, simple mixture of ex-PAN T300 carbon fibers, simple mixtures of ex-pitch FT 700 carbon fibers and $MnCl_2$, impregnated ex-pitch FT500 carbon fibers with $MnCl_2$ (ICF) and intercalation of $MnCl_2$ into ex-pitch graphitized carbon fibers P120 (GFIC). In this work, they found that the use of carbon fibers as additive no matter what sort of mixtures are used, improves kinetic results in comparison to pure $MnCl_2$. The better the additive heat conduction quality, the better the kinetic results. In addition, the higher thermal quantity leads to the prevention of agglomeration occurrence. The ICF and GFIC exhibit this character. Apart from that, they found that GFIC and ICF performed the highest energy quantity released during the exothermic reaction. Although both ICF and GFIC exhibit the best result, authors were much more concern to have ICF due to their easier preparation than GFIC and economic factor which ICF is the cheapest with sufficient degree of 'graphitization'.

As ICF is chosen the best compound, they then extent their study on parameters that can modify their heat pump performance. The parameters manipulated in designing a proper adsorber bed were: constraint pressure, constraint temperature, compression of the bed, arrangement of fibers and the contact resistance at the reactor wall. They come to a conclusion that, the influence of the first two parameters as heat pump performance increases when the difference between constraint temperature (or pressure) and equilibrium temperature (or pressure) increases. Compression influence is the most difficult to determine as, on the one hand, compression increases the bed reagent thermal conductivity which improves the reaction kinetics, and on the other hand, it reduces the refrigerant flow which diminishes the reaction rate. Therefore, the compression parameter study gave and optimal point corresponding to the best kinetic result. The arrangement of fibers influence study showed that reaction kinetics is improved when short fibers (3 cm) oriented across the diameter of a round cylindrical reactor was superior to longer fibers (30 cm) that were around the reactor center. High heat exchange coefficient value was $h = 110\,W/m^2\,K$ was due to the fact that fibers are expanding in the presence of ammonia and the contact between fibers and reactor wall is enhanced.

Fujioka et al. [32] have carried out an experiment to measure the effective thermal conductivity of beds packed with composite reactans of calcium chloride ($CaCl_2$) and functional carbon materials in order to find a simple and adequate method for heat transfer enhancement. Two kinds of composite reactans were prepared using graphite and activated carbon fiber (ACF). Expanded graphite (EG) is an extremely bulky material with $0.03\,g/cm^3$ of bulk density. The shape of expanded graphite is like a worm with about 200–300 μm in diameter and 1 mm in length, having many pores from several to dozen microns separated by thin graphite walls. Activated carbon fiber (AD'ALL) is made from a coal-tar pitch. Each fiber is about 10 μm in diameter and several milimetres in length. The common preparations were as followed:

(1) Soak and rinse the carbon material in methanol.
(2) Rinse it water and mix it with a calcium chloride aqueous solution in a beaker.
(3) Set the beaker in vacuum desiccators to concentrate the solution.
(4) Generate $CaCl_2{\cdot}2H_2O$ particles by evaporating the concentrated solution in a drier at 333 K for 30 min.
(5) Calcine and dehydrate $CaCl_2{\cdot}2H_2O$ particles in an electric furnace at 573 K for 1.0 h.

Both the ACF and EG composite beds were allowed to expand or contract in the first three reaction cycles. After the third reaction cycle was completed, the bed was compressed mildly to reduce its volume. The effective thermal diffusivity and thermal conductivity before and after compression were compared. It is observed that, the effective thermal conductivity of EG composite increased up to 10 times larger than that untreated $CaCl_2$, indicating that the heat transfer property of the bed has been improved. The effective thermal conductivity of EG composite bed before compression is about 60% as large as that of untreated $CaCl_2$. After the compression was applied, the effective thermal conductivity increased steeply with the decrease in void fraction when the overall void fraction was reduced from 0.8 to 0.7, thermal conductivity increased by three times. On the contrary, the effective thermal conductivity of ACF composite was lower than that of untreated $CaCl_2$ and no difference was observed in the dependency of thermal conductivity on void fraction before and after compression. The authors found that the steep increase in the thermal conductivity would be because the particles of EG composite are connected to each other to form the continuous path of heat flow by the compression. Reduction of the resistance for heat transfer between particles as well as that between $CaCl_2$ grain and graphite wall may contribute the increase in thermal conductivity. On the other hand, the compression seems to cause only the decease in void space between particles in the ACF composite. Such difference from EG composite would be due to the structure of ACF composite where $CaCl_2$ and carbon fibers are not mixed microscopically. By using this method, they came to conclusion that the bed volume and the overall void fraction of composite bed varied only slightly with the amount of methanol reacted, while those of untreated $CaCl_2$ bed were largely influenced by reaction. The effective thermal conductivity of expanded graphite composite bed was larger than about 60% that of the untreated calcium chloride bed under free expansion condition. When the overall void fraction was reduced to below 0.7 g by compression, the effective thermal conductivity of EG composite particle bed was sharply increased. The effective thermal conductivity of ACF composite bed was lower than the untreated $CaCl_2$ and no effect of compression on the thermal conductivity was observed.

Aidoun and Ternan [33] have examined an impregnation method to produce cobalt chloride salt crystals dispersed on carbon fibers as an alternative to intercalation technique. Ammonia was used as both the reagent for the inter-conversion of cobalt chloride salt and ammonia ($CoCl_2{\cdot}2NH_3$) and $CoCl_2{\cdot}6NH_3$ compounds and as the refrigerant. Bench scale experiments were performed using a fixed bed reactor that was weighed continuously using a load cell to obtain an instantaneous direct measurement of the salt conversion from the weight measurement. By weighing the reactor continuously throughout the course of the decomposition reaction, the conversion of $CoCl_2{\cdot}6NH_3$ salt to $CoCl_2{\cdot}NH_3$ was measured instantaneously. The salt fiber material used in the studies ($CoCl_2$ impregnated on carbon fibers) performed well. Its power densities measured during the decomposition reaction was $280\,kW/m^3$. They concluded that the salt fiber material used in this study has two advantages, i.e. large power density and its simple prepara-

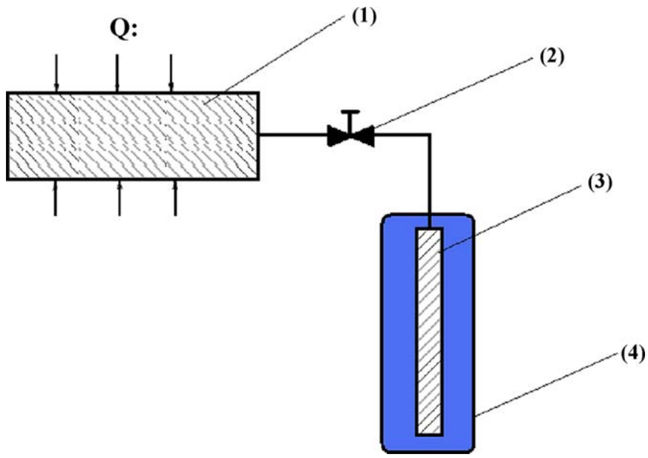


Fig. 16. Cooler based on a solid sorbent: (1) adsorber filled with an activated carbon fiber, (2) adjustable valve, (3) evaporator/condenser, and (4) vessel with a liquid. Vasiliev [35].

tion procedure compared to other materials capable of comparable power densities.

5.2. ACF composite adsorbent in cooling cycle

Vasiliev et al. [34] have designed a solar and gas solid sorption refrigerator with 1.8 m^2 collection surface. They implemented an activated carbon fiber "Busofit" saturated with different salts ($CaCl_2$, $BaCl_2$, $NiCl_2$) as a sorbent bed and ammonia as a working fluid. The main particularity of this refrigerator is consumption of solar energy with methane gas burner as a back-up. The system management consists only in actuating the special type valves to change the direction of the heating circuit and water valves to change the water cooling circuit. The ratio between solar energy and gas flame energy supply is automatically maintained on the total level of 1 kW.

For this particular design, they tested three modifications of sorbent bed in the reactor of the refrigerator. The first modification was made as a single stage system with pure adsorption ("Busofit"). The dynamic sorption capacity of this refrigerator is 0.35 kg/kg. The second modification was performed as a single stage system with complex compound sorbent bed ("Busofit" + $CaCl_2$) to combine the physical adsorption and chemical reactions in the same volume in the same time. The dynamic sorption capacity of the second modification is 0.6 kg/kg. The third modification was realized as a two-stage system ("Busofit" + $BaCl_2$ and "Busofit" + $NiCl_2$) to increase the COP due to the internal and external heat recovery. This cooling system does not need to be used with the evaporator/condenser, due to its functioning in gaseous phase, which is important for the space applications. The first prototype of the refrigerator is an adsorption machine with very short (12 min) non-intermittent cycles that uses the activated carbon fiber "Busofit" as a sorbent bed and ammonia as a working fluid. The second one is a complex compound sorbent bed ("Busofit" + $CaCl_2$) machine with the time of a cycle 25–30 min. The COP is near 0.43. The third type of the refrigerator is performed as a two-stage system with COP more than 0.44.

There is considerable scope for the application of such a hybrid gas/solar sorption systems where intermittent, or low solar insulation currently restricts their use. Such a working fluid as ammonia and energy sources like solar/gas are attractive on the environmental ground. Calculations for combined refrigeration and power-generation system operating on gas/solar energy with heat recovery show that a COP of 0.75 is achievable.

Vasiliev [35] had designed a cooler based on solid sorbents, in which an ACF and ACF impregnated with $CaCl_2$ salts and ammonia (NH_3) as the coolant are used. The system consist of an adsorber, a condenser/evaporator, and a valve that is opened in accordance with the time of the sorption–desorption cycle are shown in Fig. 16.

The condenser/evaporator is placed in a vessel (4) with cooled water. The body of the evaporator is made of stainless steel and has a diameter of 25 mm and a length of 120 mm. The body of the adsorber is made of stainless steel with diameter = 40 mm and length = 250 mm. The adsorber is filled with an activated carbon fiber dictated as sample No.1 or with a complex compound (ACF impregnated with calcium chloride $CaCl_2$) dictated as sample No. 2. The complex compound in the initial state at room temperature is impregnated with an ammonia vapor.

When the adsorber walls are heated, heat is transferred to the sorbent, and desorption occurs. The released adsorbate then enters the condenser/evaporator where it is cooled and condenses.

In the adsorber structure, aluminum fins were placed within ACF for intensifying heat exchange between the sorbent and the channel in the process of heating and cooling purposes. The maximum refrigeration output is 0.3 kW/kg for ACF sample and 0.35 kW/kg for ACF impregnated with $CaCl_2$.

6. Conclusion

Under standard nitrogen gas-(adsorption/desorption) measurement for silica gel, activated carbon (AC) and activated carbon fiber (ACF); (ACF) exhibit the best characteristics needed for a potential adsorbent. Out of many, three types of ACF tested, ACF type (A-20) is the most potential adsorbent to be implemented in cooling cycle due to its high surface area, total pore volume and average pore diameter.

Water, ammonia, carbon dioxide, acetone, methanol, ethanol and gasoline vapor are the refrigerant paired with ACF so far. All of the refrigerant mention shows good adsorption capacity when working with ACF. However, ethanol turns to be the most favorable working pair for ACF. The potential of ACF (A-20) working with ethanol are highlighted in terms of the adsorption capacity, cooling potential and the effect of bed apparent density. However, ethanol based adsorption system works under sub-atmospheric pressures.

Up to now, most researchers are focusing on employing ACF in single purpose adsorption refrigeration. Simulations and experimental work for determining COP and SCE of ACF–CO_2, ACF–methanol and ACF–ethanol were highlighted in a particular cooling cycles.

Rotary type, plate-fin tube-type and round-fin tube-type adsorber bed design have been tested. Maximum COP can be achieved by optimizing parameters involved in adsorption process. To implement ACF in plate-fin tube type, short adsorption/desorption cycle is highly suggested in order to obtain high performance. This due to the fact that the overall heat transfer coefficient of ACF in plate-fin tube type is maximum at the initial desorption process.

Composite adsorbent in chemical heat pump can reduces salt swelling and salt agglomeration phenomenon. In chemical heat pump, salt swelling reduces the heat transfer and salt agglomeration phenomenon reduces the mass transfer. Employment of additive (physical adsorbent) for chemical adsorbents could overcome these two phenomena. Employment of ACF as additive promises a bright future. Up to now, researchers have been devoted to combine ACF with metal chlorides salts in order to enhance the heat transfer in the adsorbent bed. $MnCl_2$ is favorable metal chlorides salts to be combined with ACF and out of many techniques to stick the carbon fibers to the reagent compounds, impregnated carbon fiber (ICFs) are preferred. This is due to the fact that ICFs

requires simple preparation procedure, short production time and more economical.

Calcium Chloride, Barium Chloride and Nickel Chloride are the metal salts often used with ACF when implemented in adsorption cooling cycle. Up to now, ammonia is favorable refrigerant to be paired when ACF is employed in chemical adsorbent in adsorption cooling cycle.

The practical challenge in ACF based adsorption system is the packing of the adsorbent in the assorted adsorbent beds. Further R&D work is required on simultaneous heat and mass transfer enhancements in adsorbent bed. ACF based adsorption system may lead to the use of unexploited low-temperature solar/waste heat that may offer an attractive possibility for improving energy conservation and efficiency.

Acknowledgements

The work is financially supported by the Ministry of Science, Technology and Innovation, Malaysia under the IRPA (Intensification of Research in Priority Areas). We hereby wish to acknowledge the financial assistance of the Government of Malaysia.

References

[1] Anyanwu EE. Review of solid adsorption solar refrigerator I: an overview of the refrigeration cycle. Energy Conversion & Management 2003;44:301–12.
[2] Linares-Solano A, Cazorla-Amoros D. Adsorption on activated carbon fibers. Adsorption by Carbons 2008:431–54.
[3] Saha BB, Shigeru K, El-Sharkawy II, Kuwahara K, Kariya K, Ng KC. Experiments for measuring adsorption characteristics of an activated carbon fiber/ethanol pair using a plate-fin heat exchanger. Heating, Ventilating, and Air Conditioning Research Special 2006;12(3b):767–82.
[4] Saha BB, El-Sharkawy II, Chakraborty A, Koyama S, Yoon S-H, Ng KC. Adsorption rate of ethanol on activated carbon fiber. Journal of Chemical and Engineering Data 2006;51(5):1587–92.
[5] Ryu Z, Zheng J, Wang M, Zhang B. Characterization of pore size distributions on carbonaceous adsorbents by DFT. Carbon 1999;37(8):1257–64.
[6] Alghoul MA, Sulaiman MY, Azmi BZ. Advances on multi-purpose solar adsorption systems for domestic refrigeration and water heating. Applied Thermal Engineering 2007;27:813–22.
[7] Vasiliev LL, Antux AA, Kulaov AG, Amiskinis D. Proceedings of the 19th International Congress on Refrigeration 1995;3:200–8.
[8] Vasiliev LL, Mishkinis DA, Antukh AA, Vasiliev Jr LL. Solar-gas solid sorption heat pump. Applied Thermal Engineering 2001;21:573–83.
[9] Wang RZ, Jia JP, Zhu YH, Teng Y, Wu JY, Cheng J, et al. Study on a new solid refrigeration pair: active carbon fiber-methanol. Journal of Solar Energy Engineering 1997;119:214–9.
[10] Hamamoto Y, Alam KCA, Saha BB, Koyama S, Akisawa A, Kashiwagi T. Study on adsorption refrigeration cycle utilizing activated carbon fibers. Part 1. Adsorption characteristics. International Journal of Refrigeration 2006;29:305–14.
[11] Jribi S, Chakraborty A, El-Sharkawy II, Saha BB, Koyama S. Thermodynamic analysis of activated carbon CO_2 based adsorption cooling cycles. Proceedings of World Academy of Science, Engineering, and Technology 2008;33:63–6.
[12] El-Sharkawy II, Kuwahara K, Saha BB, Koyama S, Ng KC. Experimental investigation of activated carbon fibers/ethanol pairs for adsorption cooling system application. Applied Thermal Engineering 2006;26:859–65.
[13] El-Sharkawy II, Saha BB, Kuwahara K, Koyama K, Ng KC. Adsorption rate measurement of activated carbon fiber/ethanol pair for adsorption cooling system application 2006;113:1–4.
[14] El-Sharkawy II, Saha BB, Koyama S, He J, Ng KC, Yap C. Experimental investigation on activated carbon-ethanol pair for solar powered adsorption cooling applications. International Journal of Refrigeration 2008;31:1407–13.
[15] El-Sharkawy II, Saha BB, Kuwahara K, Koyama S. Study on the fundamentals of adsorption cycle using fibrous adsorbent/ethanol pair. Nihon Dennetsu Shinpojiumu Koen Ronbunshu (CD-ROM) 2005;F324:639–40.
[16] Koyama S, Kariya K, El-Sharkawy II, Suda K, Saha BB, Kuwahara K. Numerical analysis on adsorption heat transfer of ACF/ethanol. In: Proceedings of Thermal Engineering Conference. 2005. p. 127–8.
[17] Saha BB, El-Sharkawy II, Chakraborty A, Koyama Sh, Ng KC. Study on ACF/ethanol based two stage adsorption cooling cycle; 2006. ISBN 1-56700-225-0/CD1-56700-226-9. http://www.begellhouse.com/proceedings.html [8 April 2009].
[18] Kariya K, El-Sharkawy II, Suda K, Saha BB, Kuwahara K, Koyama S. Study on adsorption process of ethanol vapor to activated carbon fibers. Transactions of the Japan Society of Refrigerating and Air Conditioning Engineers 2006;23(4):355–63.
[19] Loh WS, El-Sharkawy II, Ng KC, Saha BB. Adsorption cooling cycles for alternative adsorbent/adsorbate pairs working at partial vacuum and pressurized conditions. Applied Thermal Engineering 2009;29:793–8.
[20] Saha BB, El-Sharkawy II, Chakraborty A, Koyama S. Study on an activated carbon fiber-ethanol adsorption chiller: Part I—system description and modeling. International Journal of Refrigeration 2007;30:86–95.
[21] Saha BB, El-Sharkawy II, Chakraborty A, Koyama S. Study on an activated carbon fiber-ethanol adsorption chiller: Part II—performance evaluation. International Journal of Refrigeration 2007;30:96–102.
[22] Hamamoto Y, Alam KCA, Saha BB, Koyama S, Akisawa A, Kashiwagi T. Study on adsorption refrigeration cycle utilizing activated carbon fibers. Part 2. Cycle performance evaluation. International Journal of Refrigeration 2006;29:315–27.
[23] Yeung KH, Sumathy K. Thermodynamic analysis and optimization of a combined adsorption heating and cooling system. International Journal of Energy Research 2003;27:1299–315.
[24] Zheng A, Gu J.An advanced solar-powered rotary adsorption refrigerator with high performance. 2006. p. 3–7.
[25] Kashiwagi T, Akisawa A, Hamamoto Y, Saha BB, Koyama S, Ng KC, et al. Development of waste-heat driven multi-bed, multi-stage regenerative adsorption chiller. Final report of NEDO International Research project no:2001GP001, Japan, April 2001–2004. In: Proceedings of FY2001 International Joint Research Program (NEDO Grant) Conference. 2005. p. 190–9.
[27] Koyama S, Kariya K, Saha BB, El-Sharkawy II. Numerical analysis on the design of adsorber using ACF–ethanol pair. Nihon Kikai Gakkai Nenji Taikai Koen Ronbunshu 2006;(3):131–2.
[28] Keishi K, Tateishi R, Kuwahara K, Saha BB, Koyama S. Adsorption performance of round fin and tube type adsorber employing activated carbon fiber/ethanol pair. In: Proceedings of HT2007 ASME-JSME Thermal Engineering Summer Heat Transfer Conference. 2007. p. 829–35.
[29] Wang LW, Wang RZ, Oliveira RG. A review on adsorption working pairs for refrigeration. Renewable & Sustainable Energy Reviews 2008.
[30] Han JH, Lee KH. Gas permeability of expanded graphite-metallic salt composite. Applied Thermal Engineering 2001;21(4):453–63.
[31] Dellero T, Sarmeo D, Touzain Ph. A chemical heat pump using carbon fibers as additive. Part I: Enhancement of thermal conduction. Applied Thermal Engineering 1999;19:991–1000.
[32] Keiko Fujioka, Kensuke Hatanaka, Yushi Hirata. Composite reactants of calcium chloride combined with functional carbon materials for chemical heat pump. Applied Thermal Engineering 2008;28:304–10.
[33] Aidoun Z, Ternan M. Salt impregnated carbon fibers as the reactive medium in a chemical heat pump: the NH_3–$CoCl_2$ system. Applied Thermal Engineering 2002;22:1163–73.
[34] Vasiliev LL, Gulko NV, Khaustov VM. Proceedings of the International Sorption Heat Pump Conference, Montreal, Quebec 1996;1:3–6.
[35] Vasiliev LL. Coolers based on solid sorbents. Journal of Engineering Physics and Thermophysics 2002;75(3):706–11.
[36] Saha BB, Chakraborty A, Koyama S, Yoon S-H, Mochida I, Kumja M, et al. Isotherms and thermodynamics for the adsorption of n-butane on pitch based activated carbon. International Journal of Heat and Mass Transfer 2008;51:1582–9.